한국동력기계공학회지 제18권 제6호 pp. 186-192 2014년 12월 (ISSN 1226-7813)
Journal of the Korean Society for Power System Engineering http://dx.doi.org/10.9726/kspse.2014.18.6.186
Vol. 18, No. 6, pp. 186-192, December 2014

The Effects of Chamber Temperature and Pressure on a GDI Spray Characteristics in a Constant Volume Chamber

Seun-Sung Oh* and Seong-Soo Kim*†

(Received 31 October 2014, revised 02 December 2014, accepted 02 December 2014)

Abstract: The spray structures under the stratified and homogeneous charge condition of a gasoline direct injection were investigated in a visualized constant volume chamber. The chamber pressure was controlled from 0.1 MPa to 0.9 MPa by the high pressure nitrogen and the chamber temperatures of 25°C, 60°C and 80°C were controlled by the band type heater. The fuel, iso-octane was injected by a 6-hole injector with the pressures of 7 MPa and 12 MPa. From the experiments results, it is confirmed that at lower chamber pressure, the penetration length and spray angle are mainly affected by the chamber temperature with the vaporization of the fuel droplets and generated vortices at the end region of the spray. And at higher chamber pressure, the penetration lengths at the end of the injection were about 50~60% of that at lower chamber pressure regardless of the chamber temperature and the effect of fuel injection pressure is larger than that of the chamber temperature which results from larger penetration lengths at higher fuel injection pressure than at lower fuel injection pressure regardless of the chamber temperatures.

Key Words : Mie Scattering, Penetration Length, Spray Angle, Direct Injection, Gasoline Engine

— Nomenclature —

P_C : Chamber pressure [MPa]
Pi : Fuel injection pressure [MPa]
Tc : Chamber temperature [°C]

1. Introduction

It has been considered direct injection of fuel to combustion chamber of gasoline engines one of the major technical improvements on fuel economy in gasoline engines. The benefits of the direct-injection chemical process industry, efficient gas-liquid DISI(Direct Injection Spark Ignition) gasoline engines also includes more precise fuel mixture control and improved transient response.[1,2] Recently, a number of injector manufacturers have designed new high-pressure multi-hole injectors and outwards opening piezo injectors, referred to as 'second-generation' systems, on the expectation that they produce stable fuel sprays with fine fuel droplets independent of the time of fuel injection.[3] Multi-hole injectors have been studied due to their potential of achieving good fuel stratification, thus being able to extend the lean limit further. The investigations of multi-hole injectors for gasoline engines confirmed the improved stability of the spray at elevated chamber pressures relative to that

**† Seong-Soo Kim(corresponding author) : Department of Automotive Mechanical Engineering, Silla University.
E-mail : sskim@silla.ac.kr, Tel : 051-999-5712
*Seon-Sung Oh : Graduate School of Mechanical Engineering, Silla University.

of swirl injectors.[4] The constant high pressure chamber was equipped with high-pressure multi-hole injector at injection pressures up to 20 MPa and chamber pressures up to 1.2 MPa. The test results in the constant chamber confirmed that the overall spray angle relative to the axis of the injector was independent of injection and chamber pressure. The effects of injection and chamber pressure on droplet velocities and diameter were also quantified. Mixture preparation in direct injection engines is one of the most important processes in ensuring a successful DISI combustion system.[5]

The key to success and also the challenge in DISI engines is to prepare fuel air mixture towards the spark plug over full range of engine operating conditions according to mixture stratified and homogeneous charge modes.[6] Previous study investigated the spray structure in a constant volume chamber without temperature variation with alternative fuels.[7] In this study, to look into the detail effect of chamber temperature on the spray characteristics, the spray structures have been examined as a function of injection pressure, chamber air temperature and pressure using the Mie scattering technique under the simulated mixture charge modes.

2. Experimental setup and method

An experimental visualized constant volume chamber is shown in Fig. 1. The diameter of the visualized chamber is 130 mm and its length is 130 mm. The quartz window, the diameter of 150 mm and the thickness of 15mm is used for visualized window. The high speed camera (Fastcam SA1.1 675K Model C1) captures Mie scattering fuel spray images of 896 x 640 pixels resolutions at 10,000 frames/sec with a metal halide lamp of 250 W. The exposure time was optimized to obtain clear Mie scattering spray images. The 6-hole injector is installed at the top center of the chamber and its injection duration of 1.5 ms is controlled by the electronic control system which operates simultaneously with the Mie scattering system. But the physical injection starts at 0.4 ms ASOI and ends at 2.1 ms ASOI with a mechanical delay. The in-chamber pressure and temperature are measured by each test condition. Intake air is supplied through an intake port and exhaust gas emits through an exhaust port and its open and closing timing is controlled by high pressure solenoid valves. The fuel is supplied through the fuel line from the fuel tank of 3.5 L. The pressure of the fuel, 7 and 12 MPa is controlled by the pressure regulated nitrogen, N_2 through two high pressure

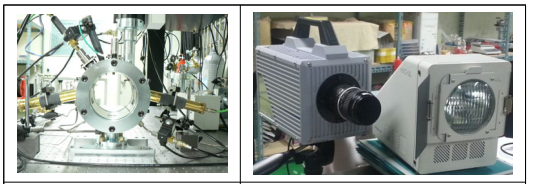

(a) Test chamber (b) Camera & lamp

Fig. 1 Mie scattering apparatus set-up

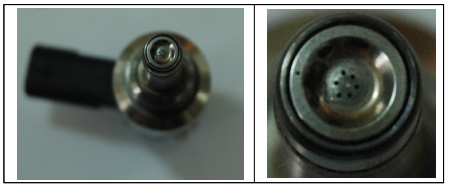

Fig. 2 Multi-hole GDI injector

Table 1 Experimental conditions

Items	Specification
Injector type	6-hole GDI injector
Chamber dia. x length	130 x 130 mm
Injection pressure	7, 12 MPa
Injection duration	1.5 ms
Chamber pressure	0.1, 0.9 MPa
Chamber temperature	25, 60, 80°C
Fuel	Iso-octane

control valves at a nitrogen bomb and a fuel tank. The temperature of chamber air can be controlled by a band type heater which enclosures the chamber outer wall. The homogeneous and stratified charge modes are simulated by the chamber pressure and temperature as shown in Table 1. The penetration length and spray angle of Mie scattering spray images are measured as shown in Fig. 3 and the averaged values of 3 raw data at each condition according to the elapsed time ASOI(After Start Of Injection).

3. Experimental results and discussion

3.1 Mie scattering spray images by chamber pressure and temperatures

The chamber pressures of 0.1 and 0.9 MPa were simulated for the simulated charge modes, homogeneous and stratified charge, and the chamber temperatures were controlled at three various temperatures such as 25°C, 60°C, and 80°C.

Fig. 4 shows Mie scattering spray images at T_c = 25°C with Pi = 7 MPa and 12 MPa according to the simulated charge modes under Pc = 0.1 and 0.9 MPa. At Pc = 0.1 MPa, the spray develops in the shape of a triangle and the jets linearly develops by elapsed time regardless of fuel injection pressure. In additions, the individual jets can be clearly distinguishable till the end of injection. At Pi = 7 MPa, the vaporization phenomena of the spray outer jets appears from 1.3 ms ASOI and the vaporizing region of outer jets increases inwardly and major outward vortices around outer jets are generated and it results from the momentum difference between vaporizing regions of jets. As the fuel injection pressure increases from 7 MPa to 12 MPa, the spray develops much actively due to the bigger momentum of jets with the increase speed of the spray penetration. But on the way of the spray development, from 1.3 ms the vortices around the end region of the spray are generated earlier than lower fuel injection pressure due to larger momentum difference between vaporizing jets. The vaporization of jets does not prompt the spray development. It is found that at 2.5 ms ASOI, the injected fuel spray departs from the tip of injector regardless of fuel injection pressure and there is a bouncing phenomena of the injector.

At Pc = 0.9 MPa, the spray develops linearly but the penetration is much smaller than that at Pc = 0.1 MPa regardless of fuel injection pressure. The difference of spray penetration between two chamber pressures increases according to the elapsed time because of the difference of fuel injection pressure and chamber pressure. The spray develops at the triangular pattern similar with lower chamber pressure condition. The jets around end region of the spray are more distinguishable than lower

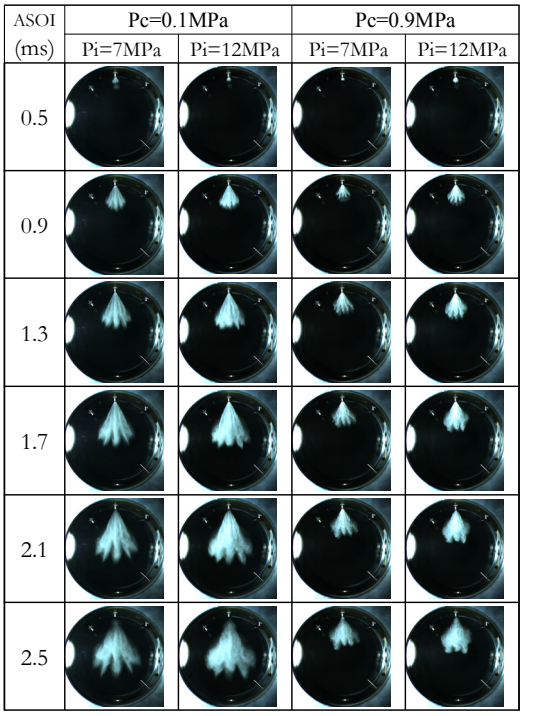

Fig. 4 Spray images at T_c = 25°C

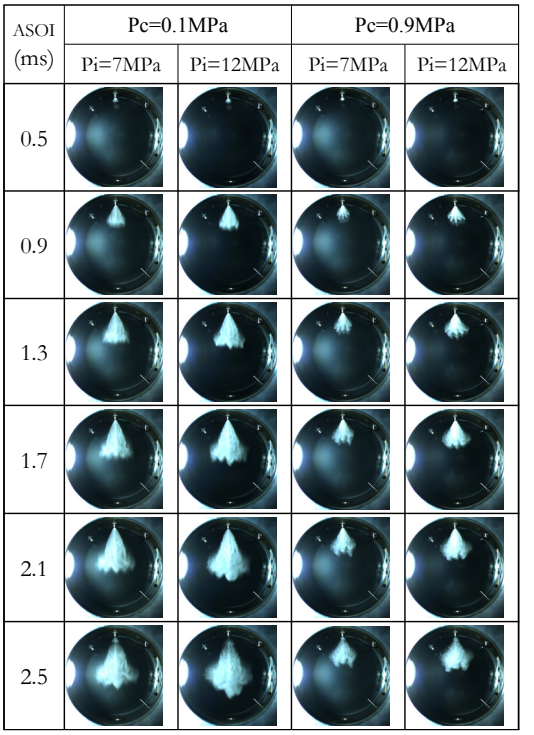

Fig. 5 Spray images at Tc = 60°C

chamber pressure condition. The generation timing of vortices at the end region of the spray is nearly same and the vaporizing region of jets is much similar with lower chamber pressure condition. At 2.5 ms the spray shapes are blunter regardless of fuel injection pressure.

Fig. 5 shows Mie scattering spray images at T_c = 60°C. Like the spray shape of Fig. 4, at T_c = 25°C, the spray develops in the shape of a triangle and the jets linearly develops regardless of fuel injection pressure. But, the individual jets can not be distinguished in the spray because the activated vaporization of jets by the elevated chamber temperature to 60°C, which caused by the agglomeration of vaporizing fuel droplets. The vaporization of the spray appears around the end region from 0.9 ms ASOI and the vaporizing region of jets increases from the end of the spray by the elapsed time and major outward vortices around outer jets are generated and it results from the momentum difference between vaporizing regions of jets. As the injection pressure increases to 12 MPa, the outward vortices around the end of the spray more actively generated due to the bigger momentum of jets and the size of vortices are much bigger compared with Fig. 4 and. spray develops much actively with the increase speed of the spray penetration. It is also found at 2.5 ms ASOI, the departure of the injected fuel spray at the tip of injector regardless of fuel injection pressure and a bouncing of the injector.

Under chamber pressure of 0.9 MPa, the spray develops linearly but the penetration is much smaller than chamber pressure of 0.1 MPa. The spray develops similarly with that of Pc = 0.1 MPa and the jets at the end region are more distinguishabletill 0.9 ms ASOI. From 1.3 ms the agglomeration of vaporizing fuel droplets and

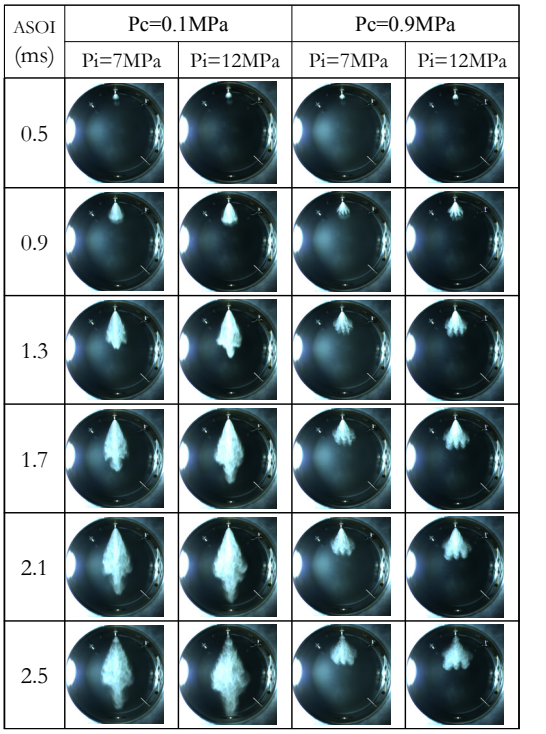

Fig. 6 Spray images at T_c = 80°C

the generation of vortices at the end region starts by the activated vaporization and the vaporizing region is relatively larger than at Pc = 0.1 MPa because of the shorter spray penetration. Therefore, from 1.3 ms ASOI, the vaporizing region occupies over two-third of the spray and from 2.1 ms ASOI, the end shape of the spray is blunter regardless fuel injection pressure.

Fig. 6 shows spray images at T_c = 80°C. The spray develops in the shape of a triangle, but at Pc = 0.1 MPa the individual jets cannot be distinguished in the spray because of the activated vaporization from 0.5 ms ASOI by the elevated chamber temperature to 80°C, which results in active agglomeration of vaporizing fuel droplets. And the vaporization and vortices generation around the end region of the spray appear clearly at 0.9 ms ASOI. The vaporizing region of the spray also increases according to the elapsed time ASOI but vortices around the outer jets as shown in Fig. 4 and 5 cannot be generated. In additions, from 0.9 ms ASOI the vaporization region of the spray enlarged and the shape around the end of the spray is much different compared with the other temperature conditions. The development of vertical direction jets of the spray is so fast that the spray is transforming in the shape of a rhombus. As the injection pressure increases from 7 MPa to 12 MPa, the rhombus shape of the spray become clearly visible from 1.3 ms ASOI and the vertical direction jets of the spray grow so rapid that the penetration length between jets enlarges till 2.5 ms ASOI.

At Pc = 0.9 MPa, the spray develops linearly but the penetration is much smaller than at Pc = 0.1 MPa regardless fuel injection pressure. The jets around the end region are more distinguishable till 0.9 ms ASOI, but from 1.3 ms the agglomeration of fuel droplets and the generation of vortices at the end region appear by the activated vaporization unlike lower chamber pressure. From 1.3 ms the vaporizing region occupies over two-third of the spray. The elevated temperature of 20°C from 60°C does not much affect on the spray structure through whole injection duration. Therefore it is found that the spray structure of 80°C are not much different from that of 60°C.

3.2 spray penetration and angle by chamber pressure and temperatures

Fig. 7 shows the penetration length and spray angle which are averaged with three measured raw data from the Mie scattering spray images at the chamber pressure of 0.1 MPa. As shown in Fig. 7(a), the penetration length of all sprays increases linearly till 2.0 ms ASOI in spite of chamber

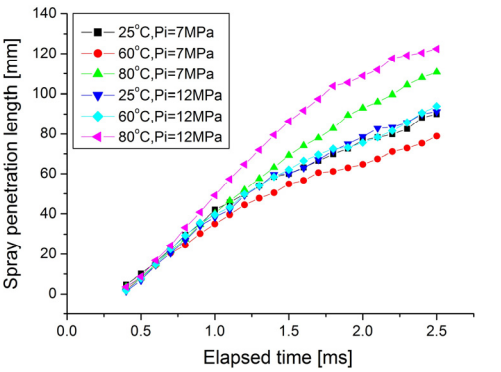

(a) Penetartion length

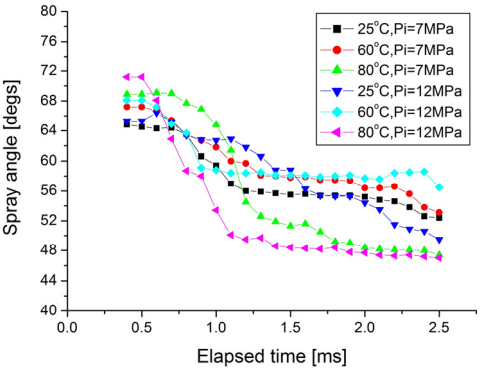

(b) Spray angle

Fig. 7 Penetration length and spray angle at Pc = 0.1 MPa

temperature difference. Therefore it is confirmed that the major parameter to affect the penetration length is chamber temperature because at high temperature condition of 80°C, the penetration lengths are longest regardless fuel injection pressure, which results from the rapid penetrating vertical direction jets. But at Pi = 7 MPa, the penetration length at Tc = 60°C is smaller than that at 25°C, which caused by the activated vaporization and vortices around the end region of the spray as shown in Fig. 5. At Tc = 25°C, the penetration length difference by the fuel injection pressure is not so much compared with the other cases. In this case, it is confirmed that the penetration lengths are not so much affected by the vaporization unlike the other

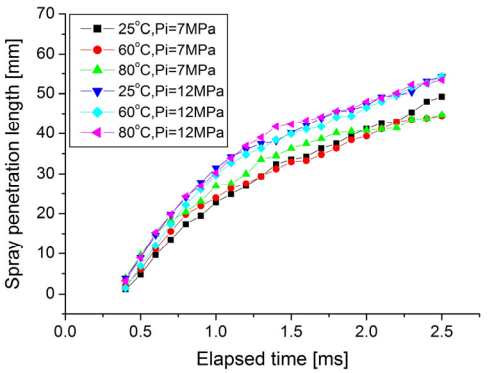

(a) Penetartion length

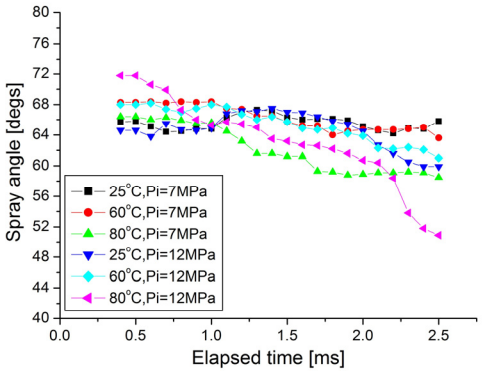

(b) Spray angle

Fig. 8 Penetration length and spray angle at Pc = 0.9 MPa

temperature conditions. And the spray angles till 0.8ms ASOI are nearly constant within the range of 64~72° and then rapid decrease happens. At Tc = 80°C, the decrease rate is biggest and the angle changes from 69~72° to under 50° due to the activated vaporization and rhombus shape spray. But at the other temperature conditions, the range of spray angle change is not so much compared with that of Tc = 80°C.

Fig. 8 shows the spray penetration and the spray angle at Pc = 0.9 MPa. At 2.5ms, the penetration length is about 50~60% of that at Pc = 0.1 MPa due to the higher chamber pressure and the major parameter to affect the penetration length is not the chamber temperature but the fuel injection pressure, because the penetration lengths at Pi = 12 MPa, are larger than at Pi = 0.7 MPa regardless the chamber temperatures. Unlike shown in Fig. 7, the vaporization of fuel droplets by elevated chamber temperature does not so much affect the spray development due to high chamber pressure. The spray angle remains constant except the case of Pi = 12 MPa and Tc = 80°C within the range of 63~69° till 1.1 ms ASOI and then there is the gradual reduction of the spray angle, except in the case of Tc = 25°C. The reduction of the spray angle can be related to the complex flow structure inside the nozzle hole, especially the presence of different types of cavitations depending on pressure difference across the nozzle.[8)]

4. Conclusions

Spray structures of a high pressure DISI multi-hole injector were examined according to the chamber temperature and pressure in a constant volume chamber using Mie scattering technique. It is confirmed that at Pc = 0.1 MPa the penetration length and spray angle are mainly affected by the chamber temperature with the vaporization of the

fuel droplets and generated vortices at the end region of the spray. And at Pc = 0.9 MPa, the effect of fuel injection pressure is larger than that of the chamber temperature which results from larger penetration lengths at high injection pressure of 12 MPa regardless of the chamber temperatures.

References

1. J. M. Nouri and J. H. Whitelaw, 2002, "Effect of Chamber Pressure on the Spray Structure from a Swirl Pressure Atomiser for Direct Injection Gasoline Engines", 1st Int. Conference on Optical Diagnostics, ICOLAD, 1, pp. 121-129.
2. G. K. Fraidl, W. F. Piock and M. Wirth, 1996, "Gasoline Direct Injection: Actual Trends and Future Strategies for Injection and Combustion Systems", SAE 960465.
3. N. Mitroglou, J. M. Nouri, M. Gavaises and C. Arcoumanis, 2006, "Flow and Spray Characteristics in Spray-Guided Injection Engines", J. Engine Res. Vol. 7, No. 3, pp. 255-270.
4. N. Mitroglou, 2005, "Multi-hole Injectors for Direct-Injection Gasoline Engines", PhD Thesis, The City University, pp. 187-248.
5. N. Mitroglou, J. M. Nouri, Y. Yan, M. Gavaises and C. Arcoumanis, 2007, "Spray Structure Generated by Multi-hole injectors for Gasoline Direct Injection Engines", SAE 2007-01-1417.
6. S. Kim, 2008, "Study on the Fuel Vapor Distribution of the Stratified Charge in a DISI Engine by PLIF Technique", KSPSE, Vol. 12, No. 6, pp. 64-69.
7. S. Kim, 2012, "The Spray Measurements of Gasoline, M85, E85, and LPG by a GDI Injector in a Constant Volume Chamber", KSPSE, Vol. 16, No. 6, pp. 5-10.
8. J. M. Nouri, N. Mitroglou, Y. Yan and C. Arcoumanis, 2007, "Internal Flow and Cavitation in a Multi-Hole Injectors for Gasoline Direct Injection Engines", SAE 2007-01-1405.